Numerical analysis of rainfall infiltration in the slope with a fracture

FAN Ping, LIU Qingquan, LI Jiachun & SUN Jianping

Division of Engineering Science, Institute of Mechanics, Chinese Academy of Sciences, Beijing 100080, China

Correspondence should be addressed to Fan Ping (email: fanping@imech.ac.cn)

Received October 14, 2004

Abstract With the finite volume method, a 2D numerical model for seepage in unsaturated soil has been established to study the rainfall infiltration in the fractured slope. The result shows that more rain may infiltrate into the slope due to existing fracture and then the pore pressure rises correspondingly. Very probably, it is one of the crucial factors accounting for slope failure. Furthermore a preliminary study has been conducted to investigate the influence of various fracture and rainfall factors such as the depth, width and location of a crack, surface condition, rainfall intensity and duration. Pore pressure and water volumetric content during the transient seepage are carefully examined to reveal the intrinsic mechanism.

Keywords: fracture slope, rainfall infiltration, numerical simulation.

DOI: 10.1360/04zze25

1 Introduction

It has been widely accepted that the rainfall infiltration through fractures is one of the most probable factors for slope failure. Recent studies have focused on the relationships between rainfall and slope failure, but the mechanisms of rainfall-induced slope failures have not been fully understood. As a result, many experiments and theoretical studies have been carried out to simulate the infiltration in the fractured soil[1—3].

Aimed at the infiltration in unsaturated rock with a single fracture, Reitsma[4] constructed a laboratory measurement on the water and oil driving experiments in water and oil flooded rock fracture made of calcareousness and obtained the relations of the capillary pressure and saturation. Romm[5] started an experiment with water and kerosene in two parallel boards to gain the laws of relative infiltration rate and saturation. The results showed that the relative infiltration rate is equal to the saturation. Through a two-phase flow experiment in natural rough-walled rock fractures, Persoff[6] found an experiential connection between relative infiltration rate and saturation. Wang[3] mathematically derived the relations between pore pressure and relative infiltration rate in a partially satu-

rated, fractured, porous medium. On the other hand, a number of models have been established to deal with the seepage in unsaturated fractured networks. Generally speaking, three kinds of models, continuum model[2,7], discrete model[8] and dual-porosity model[1], have been widely adopted for the unsaturated infiltration in the fracture networks.

In order to apply the theory to the environmental protection and disaster prevention in The Three-Gorges Dam Project in China, many valuable researches have been presented in recent years. Xu[9] proposed the super- and sub-cubic theorem and the computing model for the infiltration in the fracture networks. This research is shown to be more applicable for the analysis in the permanent gate of the Three-Gorges Dam. Zhang[10] summarized the numerical methods for the infiltration in the fractured rock. Yu[11] studied the water movement in the fractured rock and proposed a revised form for the cubic theorem. Wang[12] discussed the equivalent hydraulic width for the fractures with different roughness. With FEM, Zhang[13] simulated the rain infiltration process in the slope with one group of fracture networks. Hu[14] has compared various numerical models to offer an appropriate model more suitable for the unsaturated infiltration in fractured rock. Yao[15,16] carried a numerical simulation with the FEM to analyze the differences of the infiltration in fractured and non-fractured rocks. Huang[17] and Qi[18] simulated the infiltration in the rock with fracture respectively. Nevertheless a comprehensive review on the rules of fracture is still lacking.

Therefore, further in-depth study is still needed to understand the influences of fracture in the rock on the transient seepage and pore pressure. With a 2D unsaturated model, the present paper simulates the rainfall infiltration in the fractured slope in detail and analyzes the influences of a crack in slope with various parameters, the surface cover and different rainfall conditions on the transient seepage and pore pressure. It is expected from this research to reveal the mechanism of slope failure induced by the rainfall infiltration and provide scientific foundation for landslide management.

2 Mathematical model and numerical method

2.1 Governing equation

The rainfall infiltration on the unsaturated slope is usually regarded as an unsteady process. For the sake of simplicity, only 2D rainfall infiltration is considered in this paper. The governing equation for two-dimensional unsteady seepage flows in unsaturated soil is written as follows:

$$\frac{\partial}{\partial x}\left(K_x(H)\frac{\partial H}{\partial x}\right)+\frac{\partial}{\partial z}\left(K_z(H)\frac{\partial H}{\partial z}\right)=C(H)\frac{\partial H}{\partial t}, \tag{1}$$

in which $K_x(H)$ and $K_z(H)$ are hydraulic conductivities in the x and z directions respectively (m/s); $C(H)$ is the variation in volumetric water content per unit change in pressure head; H is the total pressure head (m), and satisfies,

$$H=h+z, \tag{2}$$

$$v = -K_z \frac{\partial H}{\partial z}, \quad u = -K_x \frac{\partial H}{\partial x}, \tag{3}$$

where h is the pore pressure or matric suction (m); and u and v are the velocity components in the x and z directions respectively (m/s).

The upper boundary condition can be divided into two kinds. When the rainfall intensity is greater than the infiltration capability of soil, the first kind of boundary condition should be adopted:

$$H|_{z=0} = \bar{H}. \tag{4}$$

As the depth of the ponding (~1 cm) is much smaller than the dimension of the computing area (~10 m), it can be regarded as zero. The second kind of boundary condition should be used when the rainfall intensity is less than the infiltration capability of the soil and no ponding on the surface:

$$K_z \frac{\partial H}{\partial z}|_{z=0} = -i, \tag{5}$$

in which i is rain intensity (m/s).

The lower boundary is set on the impenetrable layer and the boundary condition is the zero fluxes.

2.2 Discretization of the governing equation

Usually the numerical methods for the infiltration simulation include the finite difference method and finite element method. The FDM is simpler and applies for regular area only. The FEM is widely used in the problems with complicated geometry, whereas it needs more computing amount. With the finite volume method, Zhang[19] simulated the steady infiltration problem. Combining the merits of the former two methods, the FVM not only has less computing amount but also is adaptable for the complicated geometry of boundary. As a result, the current paper uses the FVM to solve the unsteady infiltration problem which is more applicable for many practical conditions.

To triangular or quadrangular cell, both the velocity components u, v and the hydraulic conductivities K_x, K_y are defined at the boundary center of the cell, while the total pressure head H and function $C(H)$ are defined at the cell center. With Green formula, the surface integral can be converted to a boundary integral as follows:

$$\iint_{\Omega_i} \left(\frac{\partial P}{\partial x} + \frac{\partial Q}{\partial z} \right) dxdz = \oint_{\partial \Omega_i} (Pdz - Qdx), \tag{6}$$

in which Ω_i is a single conjoint area, and each of the boundaries $\partial\Omega_i$ is smooth. Function $P(x, y)$, $Q(x, y)$ and its derivatives are all continuous. Hence with the above relation one can obtain

$$\iint_{\Omega_i}\left(\frac{\partial}{\partial x}\left(K_x\frac{\partial H}{\partial x}\right)+\frac{\partial}{\partial z}\left(K_z\frac{\partial H}{\partial z}\right)\right)dxdz=\oint_{\partial\Omega_i}\left(K_x\frac{\partial H}{\partial x}dz-K_z\frac{\partial H}{\partial z}dx\right)$$
$$=\iint_{\Omega_i}C(H)\frac{\partial H}{\partial t}dxdz. \tag{7}$$

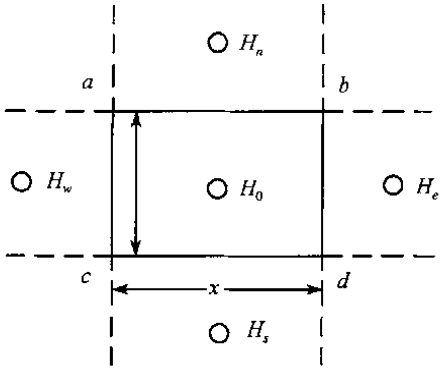

Fig. 1. Discrete scheme in space.

This equation can be discretized in space in the following ways (see Fig. 1):

$$\oint_{\partial\Omega_i}\left(K_x\frac{\partial H_0}{\partial x}dz-K_z\frac{\partial H_0}{\partial z}dx\right)=\frac{K_{x0}+K_{xe}}{2}\frac{H_e-H_0}{\Delta x}\Delta z+\frac{K_{z0}+K_{zn}}{2}\frac{H_n-H_0}{\Delta z}\Delta x$$
$$+\frac{K_{x0}+K_{xw}}{2}\frac{H_w-H_0}{\Delta x}\Delta z+\frac{K_{z0}+K_{zs}}{2}\frac{H_s-H_0}{\Delta z}\Delta x. \tag{8}$$

The temporal derivative term can be discretized by Runge-Kutta method of the second order:

$$\iint_{\Omega_i}C(H)\frac{\partial H}{\partial t}dxdz=C(H_0)\frac{\partial H_0}{\partial t}\Delta x\Delta z, \tag{9}$$

in which $\frac{\partial H_0}{\partial t}=f(t,H_0)$ and the Runge-Kutta method of second order is defined as follows:

$$\begin{cases}H_0^{n+1}=H_0^n+\dfrac{T_1+T_2}{2},\\ T_1=\Delta t\cdot f(t_n,H_0^n),\\ T_2=\Delta t\cdot f(t_n+\Delta t,H_0^n+T_1).\end{cases} \tag{10}$$

3 Influences of the fracture on the transient seepage

The fractures usually lead to increase in soil permeability. Many physical models such as the continuum model, discrete model, dual-porosity model and continuum-discrete

coupling model at present are used to determine the hydraulic conductivity of fracture. The continuum model applied in the present paper is used more widely due to its convenience. The hydraulic conductivity in the interior of a crack follows cubic theorem[9,11,12,20] looks like

$$K_c = \frac{ga^2}{12\nu}, \tag{11}$$

in which K_c denotes the hydraulic conductivity of the fracture (m/s); g is the gravitational acceleration (m/s^2); a is the width of the fracture (mm); and ν is the kinetic viscosity for water (in normal temperature it is 10^{-6} m^2/s). Thus according to the principle of discharge conservation, the soil hydraulic conductivity in a cell containing a fracture with width a should be revised as

$$K_s' = \frac{K_c a + K_s(dx - a)}{dx}, \tag{12}$$

in which K_s is the saturated hydraulic conductivity (m/s); K_s' denotes the revised saturated hydraulic conductivity (m/s); and dx is the width of the cell (m).

The relation between soil hydraulic conductivity and matric suction is experientially presented by Gardner[21] as follows:

$$K_w = \frac{K_s}{1 + 0.1\left[\dfrac{(u_a - u_w)}{\rho_w g}\right]^n}, \tag{13}$$

in which K_w is the unsaturated hydraulic conductivity (m/s), $(u_a - u_w)$ is the soil matric suction, ρ_w is the water density (kg/m^3), K_s is the saturated hydraulic conductivity (m/s), and the value of n is set as 2 in this paper. The relation between the volumetric water content and matric suction accords with experiments by Wu[22]:

$$\theta = 0.5053 - 0.0826 \lg(u_a - u_w), \tag{14}$$

in which θ is the volumetric water content. The equation is mainly applicable to the pulverous clay.

Fig. 2 shows the geometry of the slope and meshes. The whole slope ABCDE consists of three layers with different permeability. The total thickness of the slope is 30m, in which the upper layer EDIF, the middle layer FIHG, and the lower layer GHCB are 18m, 6m and 6m respectively. The permeability for the middle layer is weaker than that for the other two. The lower boundary ABC is impenetrable. MN describes a vertical fracture which starts l(m) from the slope top. The depth of this fracture is d (m). The length of the front part of the slope is 30m horizontally, while the total horizontal length of the slope is 230 m. The inclination angle of the slope in the front is 45° and 15° for the main part.

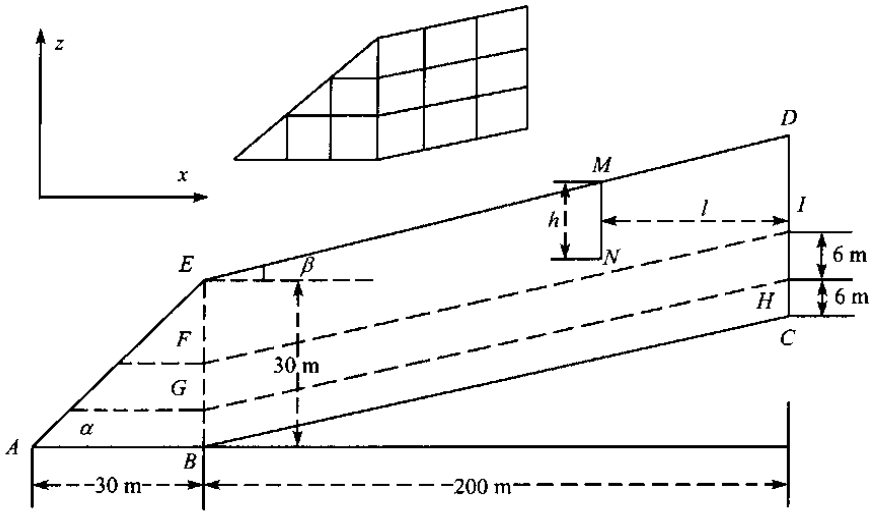

Fig. 2. Sketch for the slope dimensions and the meshes.

For the above model, the rainfall infiltration process is simulated and compared under various parameters including the depth, width and site of the fracture, the surface condition, and the rain intensity and duration. Subsequently, the influences of the parameters on the seepage and slope stability are analyzed in detail. Parameters are set as follows: the hydraulic permeability for the upper layer, middle layer, lower layer, surface and the fracture are 10^{-6} m/s, 10^{-8} m/s, 10^{-6} m/s, 10^{-7} m/s and 10^{-4} m/s respectively; the grid dimension dx and dz are 2m and 1m; the equivalent width of the crack should be 0.63 mm according to eqs. (11) and (12); l = 100 m; rain intensity is 10^{-6} m/s and duration is 5 days. Different parameters when indicated may be adopted as well.

3.1 Influence of the fracture depth

First we examine the influences of the fracture depth on the pore pressure and water volumetric content. Fig. 3(a), (b) and (c) show the results of vertical pore pressure distribution by the end of the 5th day with the depths concerned being 6 m, 18 m and 24 m respectively. We can see from these figures that with the increasing of the fracture depth, the effect of pore pressure profile can be found nearby the lower boundary of the slope. Fig. 4 compares the water volumetric content θ in the fractured soil by the end of the 5th day in four cases. For case 1 there is no fracture and only a small amount of rain infiltrates into the slope. Thus the pore pressure near the ground surface increases slightly. When the depth of fracture is 6 m, the water content in the upper layer is higher than case 1 due to enhanced penetration of water in fractured soil. However, the water content rises a little bit below the fracture. For case 3 the fracture depth is 18m where a layer with weak permeability is located, and the soil becomes saturated since the rain water accumulates there. For case 4 the fracture depth is 24 m, the water content of the bottom of the fracture has a higher value. Below the fracture the water content decreases with the depth as the hydraulic conductivity decreases.

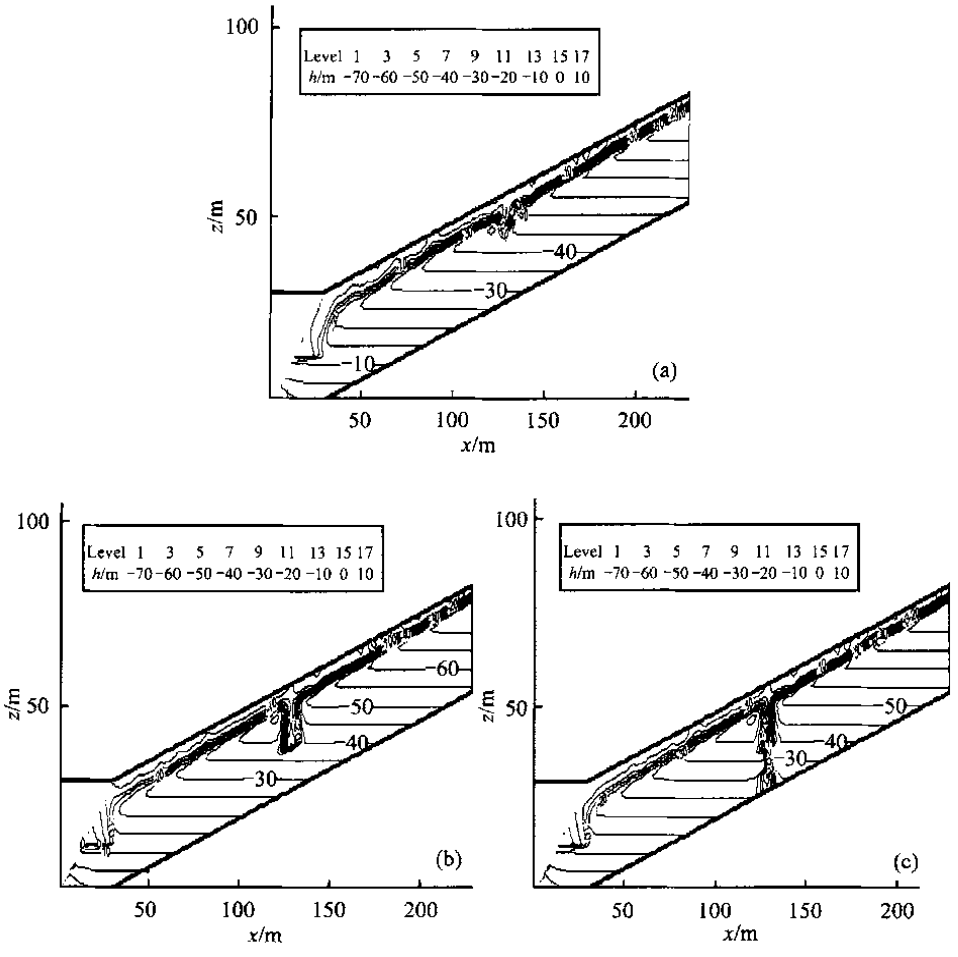

Fig. 3. Comparison of the pressure (h: m) with fracture depth being 6 m in (a), 18 m in (b) and 24 m in (c) respectively.

3.2 Influence of the fracture width

The influence of the fracture width is rather complex. According to Zhang[10], Yu[11] and Wang[12], the cubic theorem is only satisfied in a certain range of the fracture width. Therefore, the fracture width in our model should only be supposed to be in the range that the cubic theorem permits. In Fig. 5 (a) and (b) the hydraulic permeability in the crack soil are 10^{-5}m/s and 10^{-3}m/s and the equivalent fracture widths are 0.29 and 1.35 mm respectively according to eqs. (11) and (12). Comparing these two figures we may find that the bigger the fracture width, the higher the pressure. Fig. 6 gives comparison of water volumetric content θ under three kinds of fracture widths of 0.29 mm, 0.63 mm and 1.35 mm. When the fracture width is 0.29 mm, the permeability of the fractured soil is so weak that only a little rain water may infiltrate into the fracture. As a result the water content merely at the upper part of the fracture rises and decreases with the depth. As the fracture depth extends to 0.63 mm, the hydraulic conductivity of the fracture is so

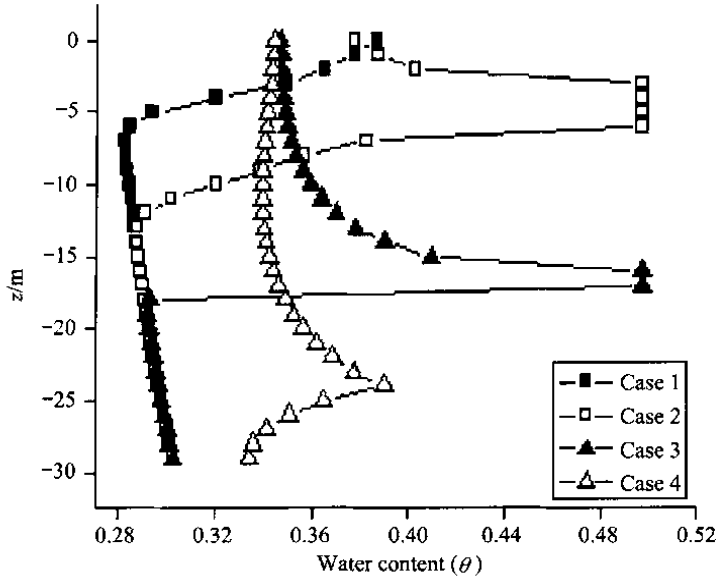

Fig. 4. Comparison of the water volumetric content θ with fracture depth 0 m, 6 m, 18 m and 24 m respectively.

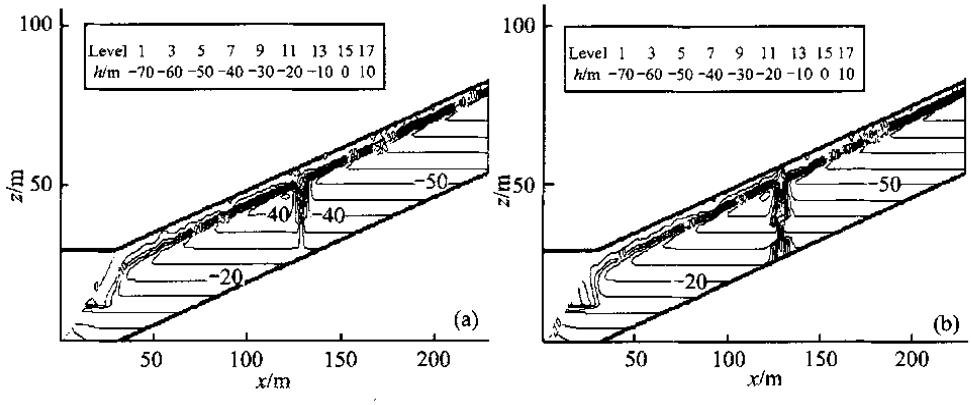

Fig. 5. Comparison of pressure (h: m) with fracture widths 0.29 mm in (a) and 1.35 mm in (b) respectively.

large that the water content rises at the fracture bottom. Thus the distribution of the water content in the vertical direction grows at first and declines subsequently. As for a 1.35 mm wide fracture the former phenomenon becomes more distinct. It can be seen that the permeability of the fracture increases with the fracture width and the water content at the bottom of the fracture reaches a maximum.

3.3 Influence of the location of the fracture

People may always find that landslide usually starts at the front of a slope, and we try to reveal the underlying mechanism. Fig. 7 (a) and (b) present the pressure distributions with a 24 m depth fracture at different locations on the slope, namely 150 m and 50

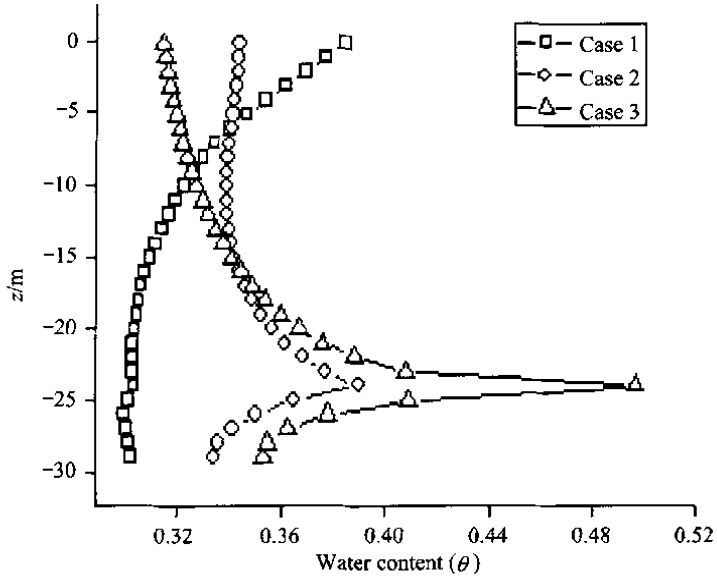

Fig. 6. Comparison of water volumetric content θ with fracture widths 0.29 mm, 0.63 mm and 1.35 mm respectively.

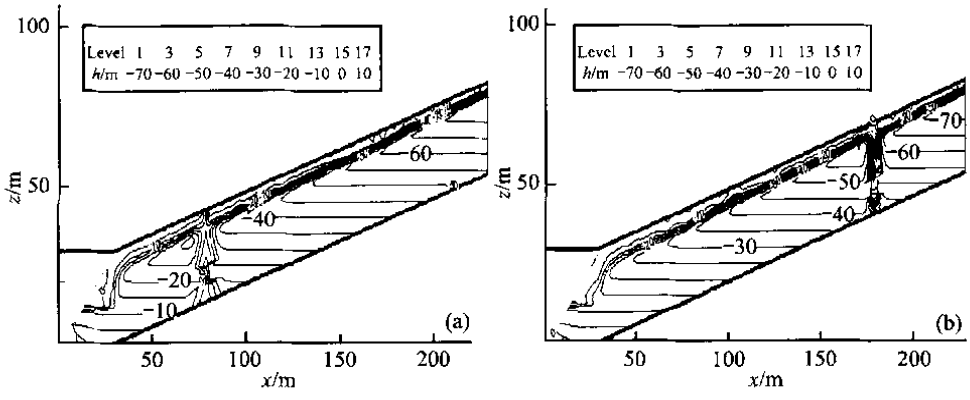

Fig. 7. Comparison of the pressure (h: m) with locations of the fracture being 150 m in (a) and 50 m in (b) respectively to top of the slope.

m from the slope top respectively. In the two figures, we find that the pressure in the fracture becomes higher as the location of the fracture moves closer to the slope front. Fig. 8 compares water volumetric content θ in the fracture by the end of 5th day in the three cases. When the distance between the location of the fracture and the slope top increases from 50 m to 100 m, the water contents at both the upper and the lower part of the fracture are increased. It demonstrates that if the runoff becomes overland flow on the slope the fracture which is located at the slope front receives more discharge from the overland flow. When the distance is 150 m, the water content value at the fracture root is the highest. On the other hand more water can infiltrate into the soil from the fracture due to the high pressure and simultaneously water in the upper part of the frac-

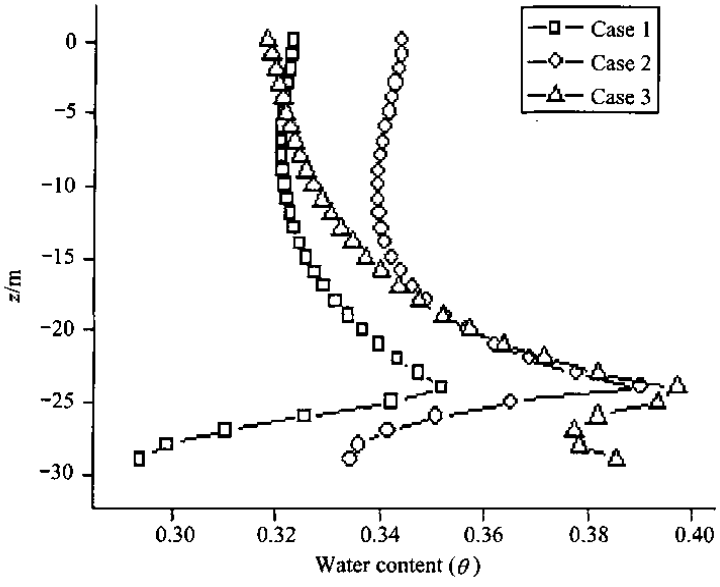

Fig. 8. Comparison of the water volumetric content θ with locations of the fracture being 50 m, 100 m and 150 m to the top of the slope respectively.

ture is fetched up to the lower part. Thus it may even decrease the water content in the upper part of the fracture. Therefore we can conclude that with the overland flow on the slope the fracture which is located at the slope front has a higher pressure value at its bottom. This is also the reason why the slope failure always starts at the slope front. It may be noted that this phenomenon cannot take place without the overland flow.

3.4 Influence of the surface condition

Sometimes the surface cover, either natural or due to human activity, forms an impeding layer and reduces the surface permeability. Fig. 9(a) and (b) show the differences of the transient pore water pressure with surface cover or not. In Fig. 9(a) the surface permeability is minimized to 1.0×10^{-7}m/s due to the surface cover, while in Fig. 9(b) it

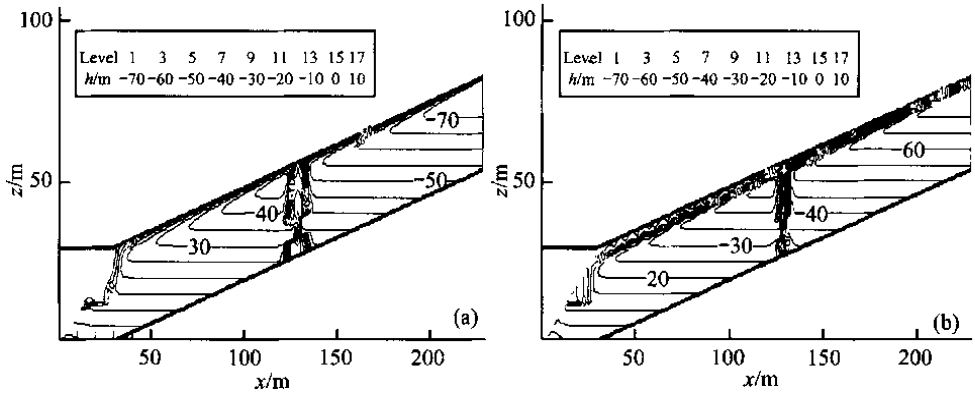

Fig. 9. Comparison of the pore pressure (h: m). In (a) with surface cover; in (b) without surface cover.

is equal to the soil permeability value 1.0×10^{-6} m/s. By comparing the two figures one can see that the pore water pressure has a wider range around the fracture with surface cover than that without surface cover. Fig. 10 presents comparison of the water volumetric content θ by the end of the 5th day with surface cover or not. We can find that the fractured soil becomes saturated for case 1 with surface cover and the water content in case 2 that without surface cover is much less. It shows that with surface cover more rainfall forms runoff, turns into overland flow and subsequently flows into the fracture. As a result, the hydraulic pressure around the fracture increases as well.

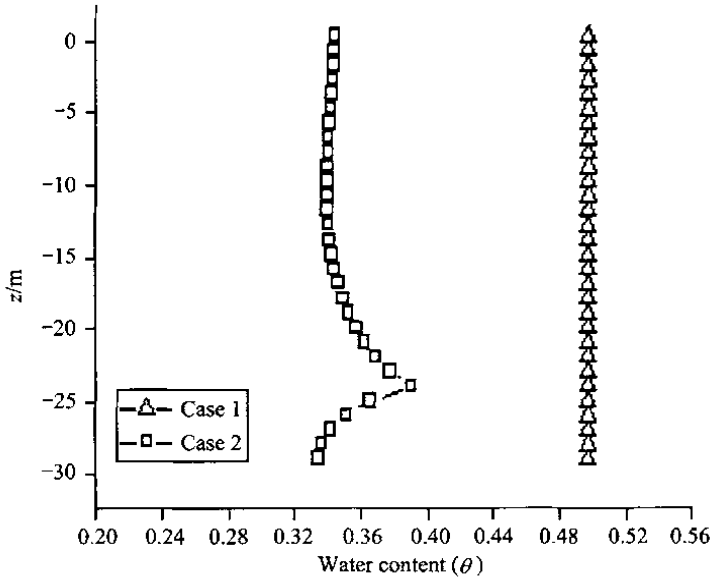

Fig. 10. Comparison of the water volumetric content θ. Case 1 with surface cover; case 2 without surface cover.

4 Transient seepages under the various rain conditions

Evidently, rain intensity and duration may exert significant influences on the transient seepage in soil and the slope stability. Therefore, the seepage in the fracture is affected greatly by the rain conditions consequently. Fig. 11(a) and (b) compare the pore pressure by the end of the 5th day for different rain intensity. The intensity of rain in Fig. 11(b) is 1.5×10^{-6} m/s (129.6 mm/d), which is triple of that in Fig. 11(a). We can see in Fig. 11(b) around the fracture the pore pressure is higher than that in Fig. 11(a). Fig. 13(a) compares the water volumetric content by the end of the 5th day under three kinds of rain intensities, which are respectively 0.5×10^{-6} m/s (43.2 mm/d), 1×10^{-6} m/s (86.4 mm/d) and 1.5×10^{-6} m/s (129.6 mm/d). We can easily find that at the lower part and the upper part of the fracture the water volumetric content increases with the rain intensity when the rain intensity increases from 43.2 to 86.4 mm/d. When the rain intensity is further enlarged to 129.6 mm/d, the soil saturates at the root of the fracture. Furthermore the higher pressure at the root of the fracture leads more water to infiltrate into the soil and consequently the water content at the upper part of the fracture may reduce.

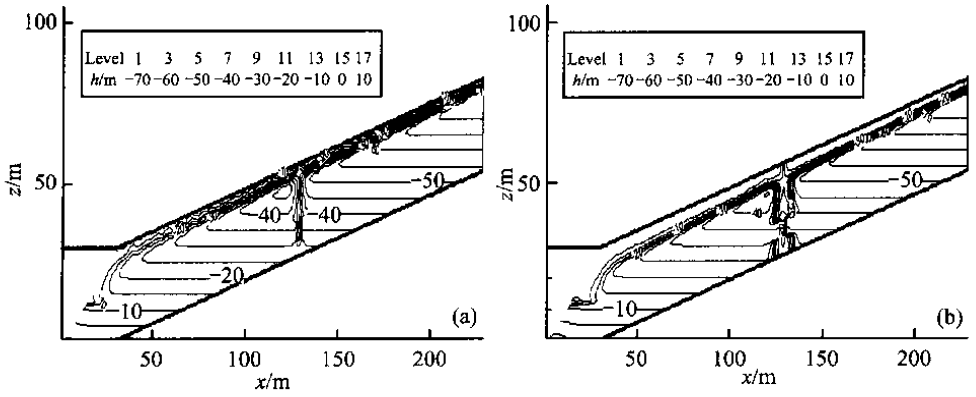

Fig. 11. Comparison of the pore pressure (h: m) with rain intensities 0.5×10^{-6} m/s in (a) and 1.5×10^{-6} m/s in (b) respectively.

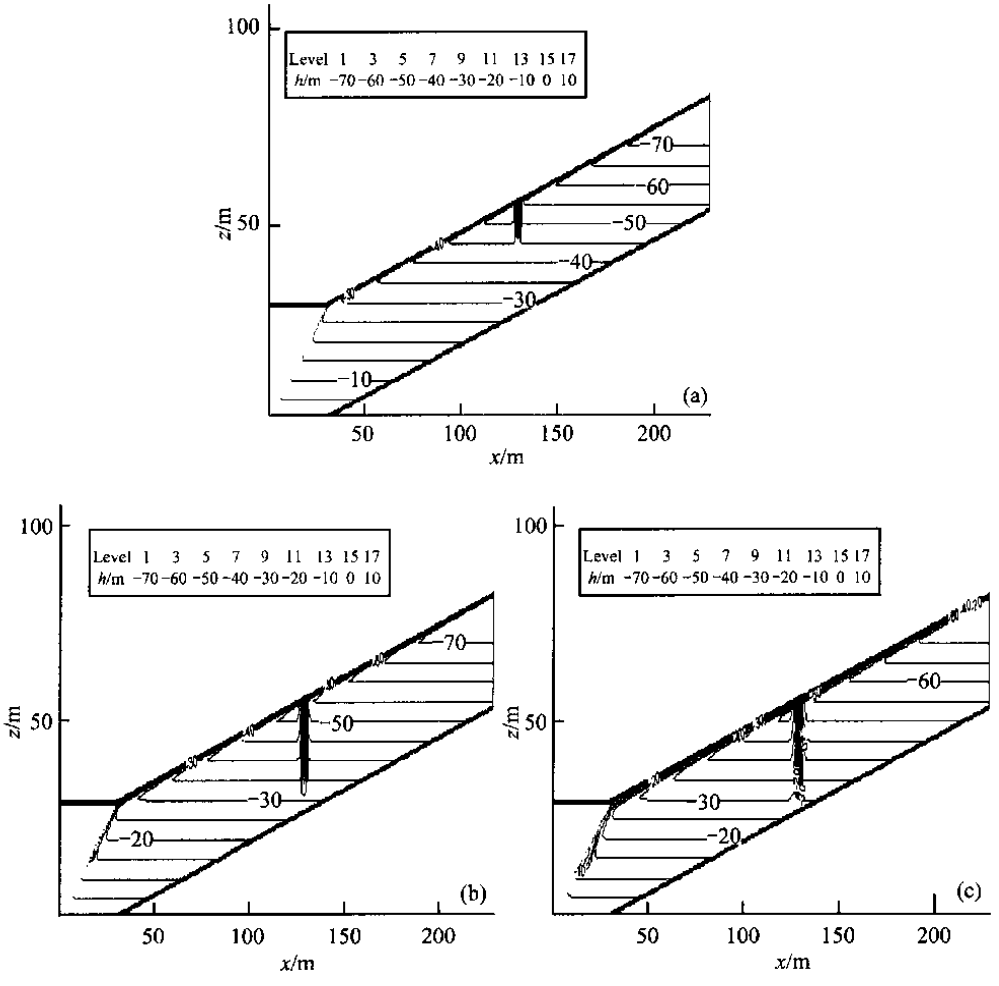

Fig. 12. Comparison of the pore pressure (h: m) with rain durations 4 h in (a), 12 h in (b) and 24 h in (c) respectively.

Fig. 12(a), (b), (c) describe the difference of the transient pore pressure under various rain durations of 4 h, 12 h and 24 h. It is obvious that the pore pressure in the fracture increases with the rain duration. Fig. 13(b) compares the water volumetric content θ under the former three rain durations. It can be seen from this figure that the area where the water content increases moves from the surface to the lower part as the rain duration increases from 4 h to 12 h. After 24 h the lower part of the fracture becomes saturated. For the same reason, the higher pressure at the root of the fracture results in more water infiltration into the soil, and the water content at the upper part of the fracture may reduce as well.

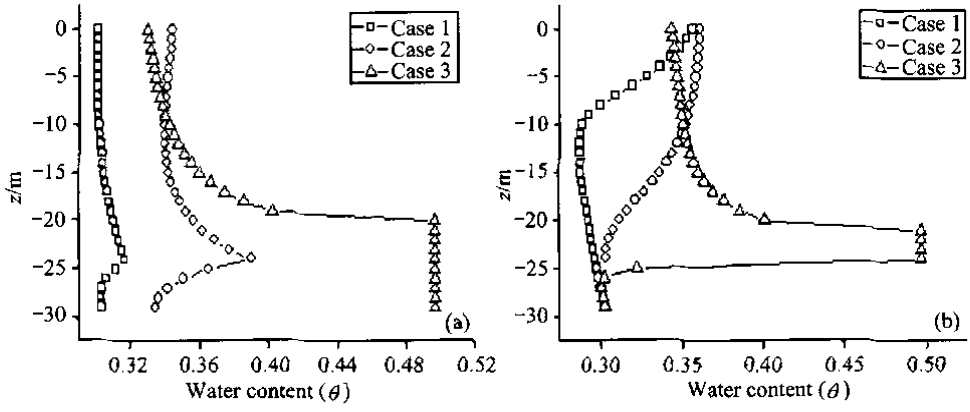

Fig. 13. Comparisons of water volumetric content θ under different rain conditions. In (a) rain intensities are 0.5×10^{-6} m/s, 1×10^{-6} m/s and 1.5×10^{-6} m/s respectively; in (b) rain durations are 4 h, 12 h and 24 h respectively.

5 Conclusions

In this paper, numerical simulations by FVM have been conducted to study the rainfall seepage in a two-dimensional fractured slope. The influences of various parameters on the seepage in the slope are carefully analyzed thus leading to the following conclusions:

1) The fractured soil exhibits higher permeability than the same soil without fracture, causing pore pressure and water volumetric content to rise locally.

2) The longer the fracture is, the deeper the effect of the fracture can reach. The permeability of the fracture grows with its width, which results in the water content increasing at the bottom and decreasing near the ground surface accordingly. If there is overland flow on the ground the pressure in the fracture close to the slope foot increases.

3) With surface cover more overland runoff may be produced and flow into the fracture which may enhance the water content in the fracture.

4) More rain infiltrates into the fracture if the rain intensity is higher and the rain lasts longer. As a result, the water content at the foot of the fracture becomes higher.

As rain infiltration into the soil changes the distribution of water content and pore

pressure in the soil, the mechanism of the slope stability and quantitative analysis should be further carried out along with the field observation.

Acknowledgements This research was supported by the "973" Project of Ministry of Science and Technology of China (Grant No. 2002CB412703), the National Natural Science Foundation of China (Grant No. 10332050), and the Knowledge Innovation Project of Chinese Academy of Sciences (Grant No. KJCX2-SW-L1-4).

References

1. Gerke, H. H., Van Genuchten, M. T., A dual-porosity model for simulating the preferential movement of water and solute in the structured porous media, Water Resour. Res., 1993, 29(2): 305—319.
2. Peters, R. R., Klavetter, E. A., A continuum model for water movement in an unsaturated fractured rock mass, Water Resour. Res., 1998, 23(3): 416—430.
3. Wang, J. S. Y., Narasimhan, T. N., Hydrological mechanisms governing flow in a partially saturated, fractured, porous medium, Water Resour. Res., 1985, 21(12): 1861—1874.
4. Reitsma, S., Kueper, B. H., Laboratory measurement of capillary pressure-saturation relationships in a rock fracture, Water Resour. Res., 1994, 30(4): 865—878.
5. Romm, E. S., Fluid Flow in Fractured Rocks (in Russian), Moscow: Nedra Publishing House, 1966, 67—95.
6. Persoff, P., Pruess, K., Two-phase flow visualization and relative permeability measurement in natural rough-walled rock fractures, Water Resour. Res., 1995, 31(5): 1175—1186.
7. Dykhuizen, R. C., Transport of solutes through unsaturated fractured media, Water Res., 1987, 21(12): 1531—1539.
8. Kwicklis, E. M., Healy, R. W., Numerical investigation of steady liquid water flow in a variably saturated fracture network, Water Resour. Res., 1993, 29(12): 4091—4102.
9. Xu, G. X. (ed.), Research on the Coupling Effect by the Seepage in the Fractured Rock and the Offload Mechanics and the Drainage in the Fracture (in Chinese), Chongqing: Chongqing University Press, 2003, 4.
10. Zhang, Q., Theory and resolve of the infiltration in the fractured rock, Advances in River and Ocean Sciences and Technologies (in Chinese), 1992, 12(4): 43—53.
11. Yu, L., Tao, T. K., Law of flow movement for rock fractures, Hydraulic and Waterborne Sciences Researches (in Chinese), 1997, 9(3): 208—218.
12. Wang, Y., Su, B. Y., Research on the behavior of fluid flow in a single fracture and its equivalent hydraulic aperture, Advances in Water Science (in Chinese), 2002, 13(1): 61—68.
13. Zhang, Y. T., Liu, Z., Saturated/unsaturated unsteady seepage analysis of rock fractured networks due to the percolation of rainfall, Chinese Journal of Rock Mechanics and Engineering (in Chinese), 1997, 16(2): 104—111.
14. Hu, Y. J., Su, B. Y., Zhan, M. L., Review of the research on unsaturated seepage flow in fractured rock masses, Journal of HoHai University (in Chinese), 2000, 28(1): 40—46
15. Yao, H. L., Zheng, S. H., Chen, S. Y., Analysis on the slope stability of expansive soils considering cracks and infiltration of rain, Chinese Journal of Geotechnical Engineering (in Chinese), 2001, 23(5): 606—609.
16. Yao, H. L., Zheng, S. H., Li, W. B., Parametric study on the effect of rain infiltration on stability of unsaturated expansive soil slope, Chinese Journal of Rock Mechanics and Engineering (in Chinese), 2002, 21(7): 1034—1039.
17. Huang, L., Zhang, A. J., Influence of precipitation-infiltration on stability of saturated fissured rock slope, Journal of HoHai University (in Chinese), 2001, 29(Supplement): 224—227.
18. Qi, G. Q., Huang, R. Q., Su, B. Y., Numeric simulation on rainfall infiltration on rock slope, Chinese Journal of Rock Mechanics and Engineering (in Chinese), 2003, 22(4): 625—629.
19. Zhang, T. F., Finite volume method of non-orthogonal mesh for analysis of seepage problems, Journal of Da-Lian University of Technology (in Chinese), 1995, 35(3): 395—399.
20. Zhou, Z. F., Wang, J. G. (ed.), Dynamics of Fluids in Fractured Media, Beijing: China Water Power Press, 2004, 1.
21. Gardner, W. R., Fireman, M., Laboratory studies of evaporation from soil columns in the presence of a water table, Soil Sci., 1958, 85(1): 244—249.
22. Wu, J. J., Wang, C. H., Li, G. X., Influence of matric suction in unsaturated soils on slope stability, Rock and Soil Mechanics, 2004, 25(5): 732—736.